Syngas/diesel dual-fuel: laminar flame speeds and engine performance

Ricardo Rabello de Castro, Pierre Brequigny, Christine Mounaïm-Rousselle

Syngas/diesel dual-fuel: laminar flame speeds and engine performance

Conference Paper · April 2021

CITATIONS
0

READS
9

3 authors:

Ricardo R. Castro
Université d'Orléans
2 PUBLICATIONS **1** CITATION
SEE PROFILE

Pierre Brequigny
Université d'Orléans
27 PUBLICATIONS **193** CITATIONS
SEE PROFILE

Christine Mounaïm-Rousselle
Université d'Orléans
186 PUBLICATIONS **3,065** CITATIONS
SEE PROFILE

Syngas/diesel dual-fuel: laminar flame speeds and engine performance

R. Rabello de Castro[1], P. Brequigny[1], C. Mounaïm-Rousselle [1]

[1]Université d'Orléans, INSA-CVL, PRISME, EA 4229, F45072 Orléans, France

Abstract

Syngas is a promising low-carbon gaseous fuel for auxiliary electricity power generation through flexible compression ignition dual-fuel IC engines. But as syngas compositions are linked to the biomass source and the different production processes, this work has as first objective to provide fundamental data, I.e. laminar flame speed, for different syngas compositions in decane/syngas mixtures as a function of initial thermodynamic conditions, with decane as the reactive fuel surrogate. Then, some initial combustion performance results, in dual-fuel operation, are presented and analyzed as a function of diesel type fuel quantity in the main syngas charge. In future work, optical experiments will be done to contribute to the understanding of the combustion process.

Introduction

The appeal of alternative fuels is strongly dependent on pressures applied by society and government policies. Biomass continues to be the main renewable energy source in Europe and is considered to be one of the solutions to achieve the EU energy targets for 2030 [1].

Syngas has been used in internal combustion engines (ICE) since the middle of the 20th century [2]. Also known as producer gas, coal gas or wood gas it can be produced by gasification of a variety of biomass. This flexibility, despite its usefulness, creates a great variability in syngas composition. Therefore, the challenge in exploring syngas as a fuel for electricity generation, relies on understanding the effect of syngas composition on combustion parameters that are relevant to engine performance and emissions.

Dual-fuel engine combustion is based on the ignition of a gaseous fuel by the direct injection of a more reactive liquid fuel, as diesel. When this injection remains a small quantity only to favor the ignition, the combustion process is called RCCI (Reactivity Controlled Compression Ignition). But in order to take full advantage of this operating mode, a better understanding of how both fuels interact during the combustion process, is still needed especially as a function of the composition of the gaseous fuel, i.e. the syngas.

One useful fundamental parameter is the laminar flame speed (S_u^0) of the fuel, which affects combustion and engine efficiencies. Most of the previous data on syngas laminar premixed flames have been focused on H_2/CO mixtures as surrogates, with the addition of some diluents [3]–[7]. But factors such as the gasifier technology, oxidizer type and biomass origin determine the product gas composition and overall quality. Therefore, the composition of syngas issued from 'real' gasifiers varies greatly with as main components H_2, CO, CO_2, N_2, and CH_4 [8].

In this study, three compositions were selected from the work of Bridgwater [8] to represent typical end-gas production of downdraft, updraft and fluidized bed (fluidbed) air-fed gasifiers (see Table 1). These are the most common and simpler types of gasifiers that do not require steam or oxygen for the gasification process. Experimental data on fundamental unstretched laminar flame speed, S_u^0 for these syngas compositions are provided in Monteiro et al. [9], [10] and recently in Rabello de Castro et al. [11]. But, to the best of the authors knowledge, no data is available on the evolution of the laminar flame speed for syngas mixed with diesel-type fuels, as it can be the case in a RCCI engine.

First, the objective of this work is to provide a comprehensive database of S_u^0 to evaluate the accuracy of available kinetic mechanisms and to help the analysis of engine performance results. For that, the classical outwardly propagating spherical flame method is used which consists of preparing the desired air/fuel mixture in a pressure and temperature-controlled vessel. Decane, ($C_{10}H_{22}$) is used as diesel fuel surrogate. Experimental S_u^0 results are compared to simulation results obtained with the kinetic mechanism of Ren et al. [12] by means of CHEMKIN PREMIX code.

Table 1: Typical syngas compositions by reactor type.

Composition	H_2 (%)	CO (%)	CO_2 (%)	CH_4 (%)	N_2 (%)
Fluidbed	9	14	20	7	50
UpDraft	11	24	9	3	53
DownDraft	17	21	13	1	48

Second, first engine combustion performance data will be presented as a function of decane fuel quantity and for the three syngas compositions.

Methodology

Laminar flame speed:

The laminar flame speed setup used here consists of an optically-accessible 4.2 L spherical vessel in which a series of flowmeters is used to simulate different mixture compositions and a high-speed Schlieren setup is used to obtain images of the propagating flame. This setup is described in depth in the following work [5], [13], [14].

The vessel has four quartz windows of 70 mm in diameter. A vacuum pump is connected to the vessel to ensure that the pressure in the beginning of the filling process is below 10 mbar. Six gaseous flowmeters deliver the air/syngas charge to the vessel while a Coriolis liquid flowmeter introduces the specified amount of decane in a mixing valve to be mixed with the gases. A fan spins in the vessel during the filling process guaranteeing homogeneity of the mixture, stopped 20 s

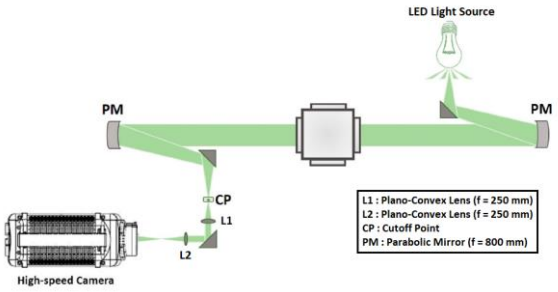

Figure 1: Schlieren optical-setup.

before the spark to avoid any turbulent motion during combustion. Several heating elements are placed along the intake line and on the vessel itself and the temperature inside the vessel is controlled by k-type thermocouples. The ignition system consists of a coil-on-plug device connected to two 0.5 mm thick electrodes with a 1.5 mm gap between them. Coil charge time is set to 3 ms resulting in a 100 mJ discharge energy. The classical Z-Schlieren optical setup, schematized in Figure 1: Schlieren optical-setup. images, with a high-speed Phantom V1610 camera, set at 7000 frames per second with a spatial resolution of 0.11 mm/pixel. The post-processing is done in the Matlab environment and consists of obtaining the flame contour and equivalent radius over time profile, as more detailed in Di Lorenzo et al. [13]. The non-linear extrapolation method is used to provide the unstretched burning velocity value. Uncertainties presented are calculated based on the work of Brequigny et al. [15] . Overall uncertainty values are the combination of statistical, hardware related (3.5 %) and imaging (2.5 %) errors.

Measurements were made at 1, 3 and 5 bar absolute initial pressure and the initial temperature was 423 K (to avoid condensation). Syngas/air equivalence ratio was increased gradually from 0.5 to the point where the flame was unstable. The decane fractions are given as the ratio between decane and total fuel in the vessel as given in Eq.(1).

$$Decane_{\%} = 100.\frac{Decane_{mass/vol/energy}}{Decane_{mass/vol/energy} + Syngas_{mass/vol/energy}} \quad (1)$$

Table 2: Mixture configurations for laminar flame speed measurements.

Syngas + Decane content (mass %)	Decane content (vol. %)	Decane content (energy)	Syngas/air Equivalence Ratio	Global Equivalence Ratio range
Downdraft + 2.5%	0.45	19.0	0.5- 1.2	0.67– 1.6
Updraft + 2.5%	0.46	17.6	0.5- 1.2	0.65– 1.57
Fluidbed + 2.5%	0.49	17.8	0.5– 1.0	0.65– 1.3
Downdraft+ 5%	0.90	32.4	0.5– 1.0	0.83– 1.66
Updraft + 5%	0.92	30.5	0.5- 1.0	0.8– 1.57
Fluidbed + 5%	0.98	30.7	0.5- 0.9	0.8– 1.44

Engine setup:

The engine setup consists of DW10 PSA engine converted to single-cylinder, with classical Mexican hat bowl design. The main engine characteristics are given in Table 3.

Table 3: Engine characteristics.

Displaced Volume	499 cm³
Bore	85 mm
Stroke	88 mm
Connecting Rod	145 mm
Compression Ratio	15.7
Swirl Ratio	1.1
Engine Speed	750 rpm

The engine intake charge is controlled by six gaseous flowmeters for the air and the 5 components of the syngas mixtures. Injection is achieved through a common-rail system set a reduced pressure of 200 bar in order to achieve small pilot fuel quantities. The injector used was a Bosch CRI 2.2 with six 0.13 µm holes at a 149º umbrella angle. The injector characterization was realized through the Bosch injection rate method. In-cylinder pressure was measured with a Kistler 6043A piezo-electric pressure sensor (accuracy of ± 2%). Temperature and pressure at the intake were set to 25 ºC and 1 bar respectively. Testing procedure consisted of establishing a baseline at 5.5 bar of Indicated Mean Effective Pressure (IMEP) with only decane as fuel with a stability of 5% (CovIMEP). From this point, the amount of syngas in the intake and the pilot injection are adjusted to maintain the IMEP constant.

Results and discussion

Laminar flame speed.

In Figure 2, first average results of flame speed for pure decane, with uncertainty intervals, are plotted and compared with those available in literature at similar temperatures conditions. Both Munzar et al. [16] and Ji et al. [17] results are globally within the present uncertainty intervals but with less accuracy for richer mixtures. Maximum flame speeds are all within 5% of each other and are reached at around 1.05-1.1. The simulation results are globally close to experimental data, but the present data is closer for rich mixtures.

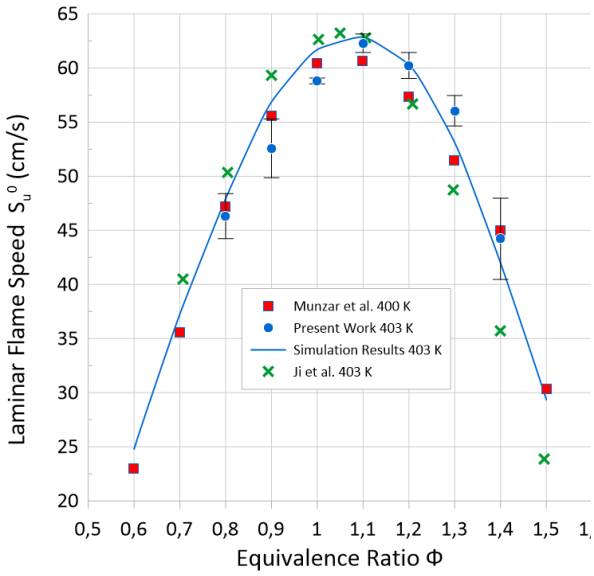

Figure 2: Comparison of decane/air laminar flame speeds results at 1 bar. Simulation results: continuous line (403K)

In Figure 3, S_u^0 is plotted over syngas/air equivalence ratio (without the added decane fuel) for 3 contents of decane (0, 2.5 and 5% mass fractions) and for the 3 syngas compositions. For reference, a 2.5% case corresponds to a 33% greater global equivalence ratio than syngas/air equivalence ratio (see Table 2). The shift in maximum flame speed location (present for all 3 compositions) is the result of this change in global equivalence ratio. As a reminder, the downdraft, updraft and fluidbed compositions are the ones with the highest H_2, CO and CO_2 contents respectively (see Table 1). Results show a good agreement between experimental and simulation results. In the case of downdraft/air flames with decane addition the mechanism tends to over-predict S_u^0 for richer mixtures. This is consistent with Figure 2 where results from Ji et al. [17] and the simulation results diverge.

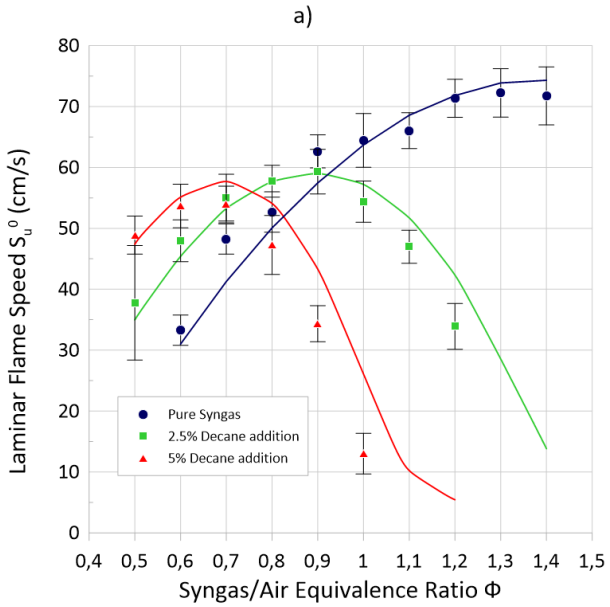

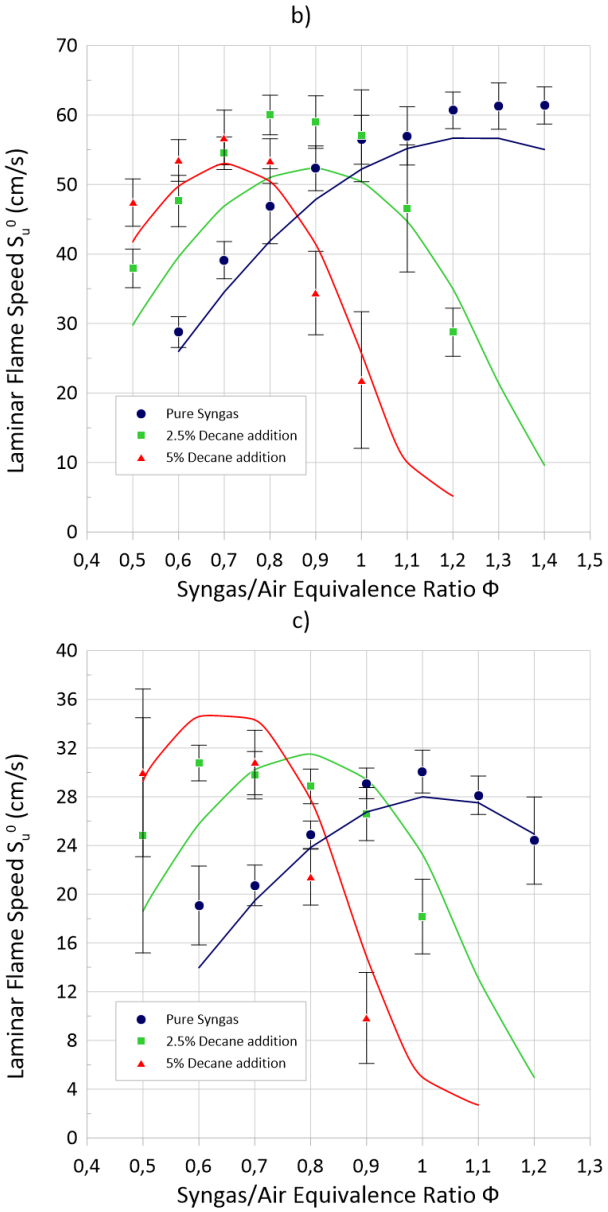

Figure 3: evolution of laminar flame speed as a function of syngas/air equivalence ratio for 3 decane contents at 1 bar and 423 K. a- downdraft composition, b- updraft, c- fluidbed syngas composition, simulation results in continuous line.

In the case of the Fluidbed/air flames in Fig.3c the higher experimental uncertainties make it more difficult to evaluate the accuracy of the mechanism.

*Figure 4***Erreur ! Source du renvoi introuvable.** presents the effect of the initial pressure on the maximum unstretched laminar flame speeds of decane/syngas/air flames with 2.5 and 5% of decane. Results show that, globally, the same behavior is obtained for all syngas compositions: a decrease near 40% is obtained for a pressure increase from 1 to 5 bars, but with lower absolute value for the fluidbed composition, which can affect strongly the combustion process in engine combustion chamber.

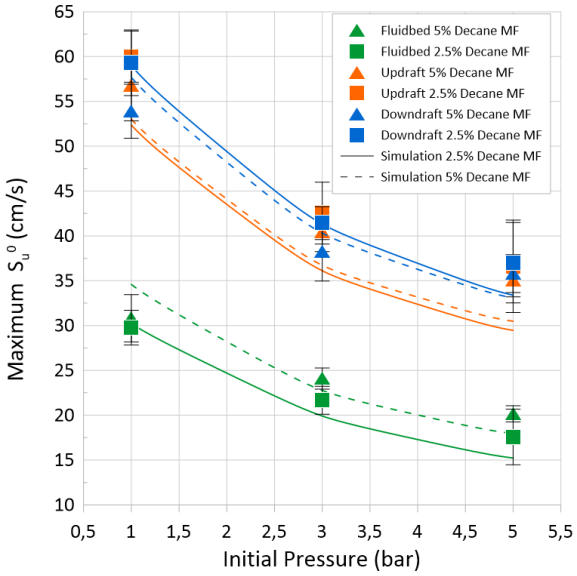

Figure 4: Effect of pressure on maximum laminar flame speed.

A few key conclusions can be drawn from the laminar flame speed results presented here:

- The addition of decane in syngas/air flames can increase S_u^0 for lean mixtures, even surpassing the maximum pure syngas values in the case of fluidbed composition;
- Similar effect of pressure in maximum S_u^0 was obtained;
- Higher H_2 content on the downdraft composition produces faster flames whereas, low H_2 and CO combined with high CO_2 content (in the case of fluidbed) produces slower flames (almost half of the speed).
- Ren et al. mechanism predict globally the laminar flame speed values but accuracy is worse for updraft and at higher pressures S_u^0 is underpredicted.

Engine performance results

Figure 5 presents the in-cylinder pressure as a function of the crank angle (CAD) for 2 syngas/air equivalence ratios (0.5 and 0.7) for the 3 syngas compositions. Pure decane result is plotted as reference. The quantity of decane and the injection timing (IT, in the figure) were adjusted to keep constant the IMEP varying intake charge equivalence ratio (See Table 4).

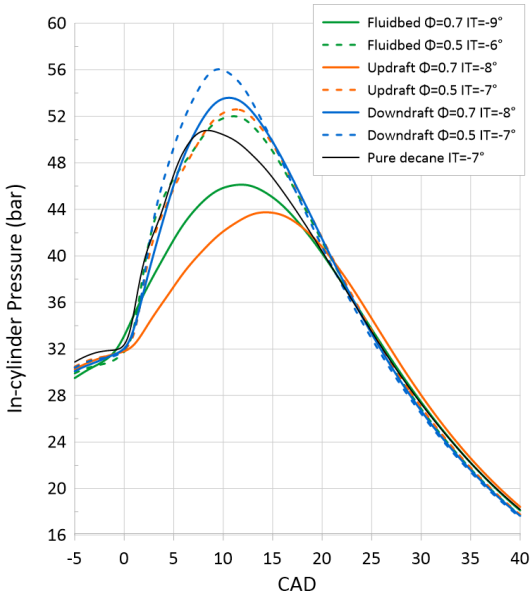

Figure 5: In-cylinder pressure as a function of crank angle for 2 syngas/air equivalence ratios and the 3 syngas compositions.

In the case of the syngas equivalence/ratio of 0.5, the maximum in-cylinder pressure is higher when compared to the decane only case. In all cases the peak pressure crank angle is delayed by adding syngas to the intake charge despite the injection timing compensation. Increasing the premixed equivalence ratio decreases this maximum pressure for all compositions and more strongly with the fluidbed and updraft ones.

In Figure 6Figure 6, one can note the peak of the heat release rate (RoHR) is higher for Φ= 0.5 than the case without syngas in the charge. The combustion development presents at least two phases: a fast one, with highest heat release rate, like HCCI combustion and a second one, more continuous without important peak, contrary to the case of pure decane. When Φ= 0.5 is increased to Φ= 0.7, the combustion becomes globally slower with a single-phase, similar to classical combustion development in spark-ignition engine. Regarding RoHR peak, the highest values were achieved with the downdraft mixture which is consistent with S_u^0 results. In the case of the fluidbed composition, despite of its lower laminar flame speed, its combustion development is similar to the updraft one.

Table 4 summarizes the different combustion phasing (CAXX corresponding to the crank-angle degree when X% of fresh gases is burnt) as a function of syngas amount in the 5.5 bars of IMEP. RLFC is the reduction of liquid fuel (here decane) consumption. First, it was possible to maintain the same IMEP target, by replacing at least 90% of decane by syngas for all syngas compositions. Second, as expected more the less reactive fuel (syngas) amount is, more the combustion is delayed, as represents the difference of CA10 (combustion onset)

and the IT (start of injection), without identifiable impact of syngas compositions. Therefore, the injection timing had to be advanced with the syngas/air equivalence ratio increase.

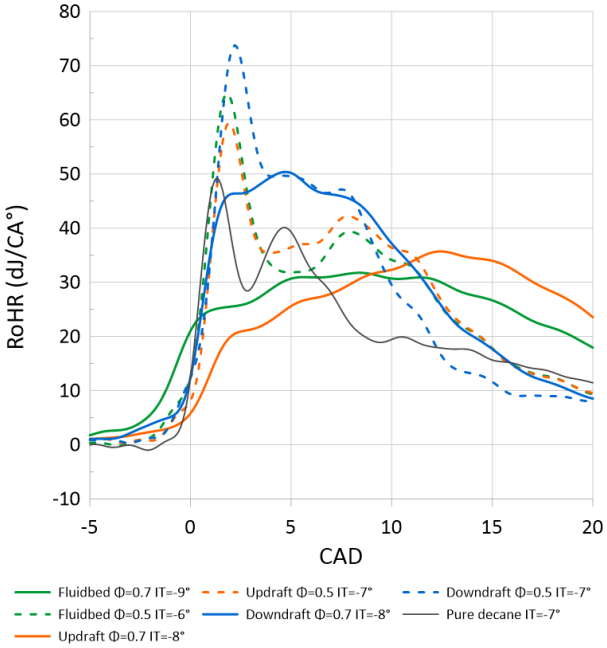

Figure 6: apparent heat release rate for 2 syngas/air equivalence ratios and 3 syngas compositions.

Table 4: Combustion phasing results for varying intake charge equivalence ratios.

	Φ_{premix}	Φ_{global}	IT	RLFC (%)	CA10	CA50
Decane Only	0	0.5	-7	0	2.3	10.6
Downdraft	.05	0.51	-7	10	2.1	10.9
	0.1	0.52	-7	19	2.3	11.6
	0.3	0.58	-8	49	1.6	9.5
	0.5	0.68	-8	68	1.7	7.7
	0.7	0.76	-9	90	1.6	8.5
Updraft	.05	0.53	-7	7.3	2.1	11.1
	0.1	0.54	-7	17	2.1	11.3
	0.3	0.57	-7	51	2.4	11.4
	0.5	0.64	-8	76	1.9	9.4
	0.7	0.71	-8	98	3.6	14
Fluidbed	.05	0.52	-6	8.3	3	11.3
	0.1	0.51	-6	21	3.3	12.2
	0.3	0.57	-7	49	2.4	11.1
	0.5	0.63	-9	75	1.6	9.2
	0.7	0.72	-12	96	1.7	12

Figure 7: Combustion timings evolution with premixed equivalence ratio. synthesizes the different phases of the combustion development (from data in Table 4: the ignition delay (CA10-IT) and the first phase of flame development CA50-CA10). The increase of syngas content increases the ignition delay, similarly for all compositions until Φ_{premix}=0.5 but where the effects of the different flame speeds induce sharper increase for fluidbed and updraft when compared to downdraft. On the other hand, the combustion duration seems to decrease until Φ_{premix}=0.5 with a sharp increase from Φ_{premix}=0.5 to Φ_{premix}=0.7 (consistent with Figure 6). This is due to the fact that, the injection timing was not advanced further from Φ_{premix}=0.5 to Φ_{premix}=0.7 in order to keep the IMEP from going over 5.5 bar.

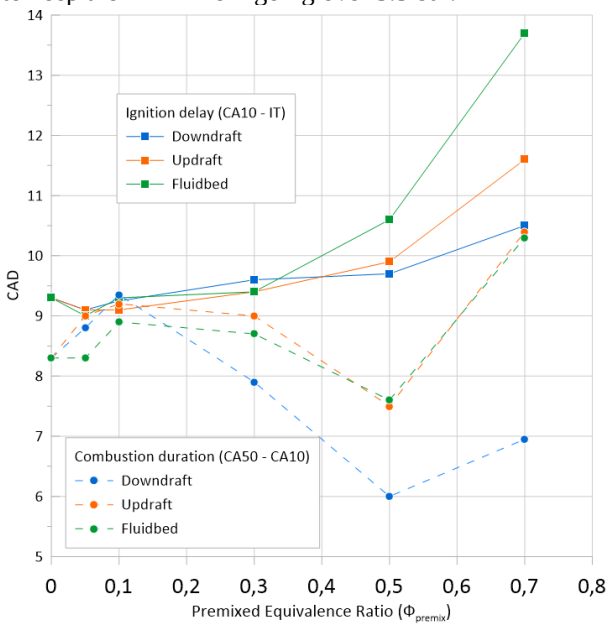

Figure 7: Combustion timings evolution with premixed equivalence ratio.

Conclusions

This study provided new unstretched laminar flame speeds of three syngas compositions (representing three types of gasifiers) with the addition of decane fuel as diesel surrogate to be representative to RCCI combustion. The addition of decane increases laminar flame speeds for lean syngas/air mixtures. In the case of the fluidbed composition the small addition (2.5% in mass) is sufficient to raise maximum flame speeds above those found with fluidbed/air only. The kinetic mechanism of Ren et al. [12] was chosen to simulate laminar flame to compare with the experimental results. The overall accuracy of the mechanism was globally

satisfactory but it tends to underpredict S_u^0, especially for updraft and fluidbed syngas at ambient conditions and for all syngas compositions, at higher pressures. This performance has to be evaluated considering the fact that the mechanism was optimized for C_7 and higher hydrocarbons and not the specific mixtures studied here.

Operation with different syngas compositions and small pilot injection of decane was achieved in a single-cylinder CI engine. The introduction of syngas increases the heat release rate peak when the decane injection timing and quantity are optimized to maintain same engine output energy and stability. The ignition delay increases with syngas amount increase, requiring the injection timing advance. Over 90% of the fuel used in the reference decane-only case can be replaced by syngas whilst maintaining the same power output for any syngas compositions.

Following this study, optical diagnostics (such as fuel tracer-PLIF and chemiluminescence) will be used in order to improve understanding of the interaction between the decane liquid injection and the premixed syngas/air charge and the combustion development.

Acknowledgement

The research leading to these results has received funding from the French Government's "Investissement d'Avenir" program: "Laboratoire d'Excellence CAPRYSSES" (Grant No ANR-11-LABX-0006-01) and Région Centre Val de Loire.

References

[1] European Commission, "Brief on biomass for energy in the European Union," *EC Publ.*, pp. 1–8, 2019.

[2] F. Y. Hagos, A. R. A. Aziz, and S. A. Sulaiman, "Trends of syngas as a fuel in internal combustion engines," *Adv. Mech. Eng.*, vol. 2014, 2014.

[3] C. Prathap, A. Ray, and M. R. Ravi, "Investigation of nitrogen dilution effects on the laminar burning velocity and flame stability of syngas fuel at atmospheric condition," *Combust. Flame*, vol. 155, no. 1–2, pp. 145–160, 2008.

[4] Y. Xie *et al.*, "A comprehensive review on laminar spherically premixed flame propagation of syngas," *Fuel Process. Technol.*, vol. 181, no. September, pp. 97–114, 2018.

[5] N. Bouvet, C. Chauveau, I. Gökalp, and F. Halter, "Experimental studies of the fundamental flame speeds of syngas (H 2/CO)/air mixtures," *Proc. Combust. Inst.*, vol. 33, no. 1, pp. 913–920, 2011.

[6] S. Wang *et al.*, "Experimental and numerical study of the e ff ect of elevated pressure on laminar burning velocity of lean H 2 / CO / O 2 / diluents fl ames," *Fuel*, vol. 273, no. April, p. 117753, 2020.

[7] R. Shang, Y. Zhang, M. Zhu, Z. Zhang, D. Zhang, and G. Li, "Laminar flame speed of CO2 and N2 diluted H2/CO/air flames," *Int. J. Hydrogen Energy*, vol. 41, no. 33, pp. 15056–15067, 2016.

[8] A. V. Bridgwater, "The technical and economic feasibility of biomass gasification for power generation," *Fuel*, vol. 74, no. 5, pp. 631–653, 1995.

[9] E. Monteiro, M. Bellenoue, J. Sotton, N. A. Moreira, and S. Malheiro, "Laminar burning velocities and Markstein numbers of syngas-air mixtures," *Fuel*, vol. 89, no. 8, pp. 1985–1991, 2010.

[10] E. Monteiro and A. Rouboa, "Measurements of the laminar burning velocities for typical syngas-air mixtures at elevated pressures," *J. Energy Resour. Technol. Trans. ASME*, vol. 133, no. 3, pp. 1–7, 2011.

[11] R. R. De Castro, P. Brequigny, J. P. Dufitumukiza, and C. Mounaım-Rousselle, "Laminar flame speed of different syngas compositons for engine relevant conditions [manuscript submitted for publication]," *Fuel*, 2021.

[12] S. Ren, S. L. Kokjohn, Z. Wang, H. Liu, B. Wang, and J. Wang, "A multi-component wide distillation fuel (covering gasoline, jet fuel and diesel fuel) mechanism for combustion and PAH prediction," *Fuel*, vol. 208, pp. 447–468, 2017.

[13] M. Di Lorenzo, P. Brequigny, F. Foucher, and C. Mounaïm-Rousselle, "Validation of TRF-E as gasoline surrogate through an experimental laminar burning speed investigation," *Fuel*, vol. 253, no. September 2018, pp. 1578–1588, 2019.

[14] B. Galmiche, F. Halter, and F. Foucher, "Effects of high pressure, high temperature and dilution on laminar burning velocities and Markstein lengths of iso-octane/air mixtures," *Combust. Flame*, vol. 159, no. 11, pp. 3286–3299, 2012.

[15] P. Brequigny, H. Uesaka, Z. Sliti, D. Segawa, F. Foucher, and G. Dayma, "Uncertainty in measuring laminar burning velocity from expanding methane-air flames at low pressures," in *11th Mediterranean Combustion Symposium*, 2019, no. June, pp. 16–20.

[16] J. D. Munzar, B. Akih-Kumgeh, B. M. Denman, A. Zia, and J. M. Bergthorson, "An experimental and reduced modeling study of the laminar flame speed of jet fuel surrogate components," *Fuel*, vol. 113, pp. 586–597, 2013.

[17] C. Ji, E. Dames, Y. L. Wang, H. Wang, and F. N. Egolfopoulos, "Propagation and extinction of premixed C5-C12 n-alkane flames," *Combust. Flame*, vol. 157, no. 2, pp. 277–287, 2010.